Novel synthesis of magnetic poly(cyclotriphosphazene-*co*-4,4′-sulfonyldiphenol) nanotubes with magnetic phases embedded in the walls†

Xiaoyan Zhang,[a] Xiaobin Huang*[a] and Xiaozhen Tang*[ab]

Received (in Victoria, Australia) 2nd July 2009, Accepted 3rd August 2009
First published as an Advance Article on the web 27th August 2009
DOI: 10.1039/b9nj00300b

Magnetic poly(cyclotriphosphazene-*co*-4,4′-sulfonyldiphenol) (PZS) nanotubes with magnetic phases embedded in the walls were synthesized by ultrasonic irradiation *via* an *in situ* template approach. The structure and morphology of the magnetic PZS nanotubes were determined by FT-IR, XRD, FE-SEM, HR-TEM and EDX spectroscopies. The characterization results show that the magnetic PZS nanotubes are 50–100 nm in outer diameter and 5–10 nm in inner diameter; the Fe_3O_4 nanoparticles with diameter of 5–10 nm are embedded in the walls of the nanotubes. The morphology of the magnetic PZS nanotubes is greatly influenced by the content of Fe_3O_4 nanoparticles. A possible formation mechanism of the magnetic PZS nanotubes is proposed. The TGA results and the magnetic measurements show that the magnetic PZS nanotubes have good thermal stability and superparamagnetic properties.

Introduction

Over the past few years, magnetite (Fe_3O_4) nanoparticles have attracted great interest because of their strong magnetic responsiveness and wide applications in magnetic fluids, catalysis, biotechnology, magnetic resonance imaging, data storage, and environmental remediation.[1–4] At present, many researchers are paying much attention to the study of combining magnetite nanoparticles with nanotubes for a wide variety of applications.[5–7] Korneva *et al.*[8] produced magnetic nanotubes by filling carbon nanotubes with paramagnetic iron oxide nanoparticles *via* chemical vapor deposition. Son *et al.*[9] synthesized silica nanotubes with a layer of Fe_3O_4 nanoparticles on the inner surface of the nanotubes using porous alumina film as a template. However, the studies are basically focused on inorganic nanotubes such as carbon nanotubes[8,10–13] and silica nanotubes[9,14] with magnetite nanoparticles either attached on the outer surface or encapsulated inside the hollow structure. Few of these studies are researching magnetic polymer nanotubes. Compared with inorganic nanotubes, polymer nanotubes have the advantage of light weight, low-cost, flexibility and tunable structure. Recently, we have reported novel magnetic phosphazene-containing polymer nanotubes with magnetic nanoparticles attached on the outer surfaces,[15] which exhibit excellent properties.

Here, in this work, we synthesized novel magnetic poly(cyclotriphosphazene-*co*-4,4′-sulfonyldiphenol) (PZS) nanotubes with magnetic phases embedded in the walls *via* an *in situ* template approach. The magnetite nanoparticles take part in the formation of the magnetic nanotubes together with cyclotriphosphazene and 4,4′-sulfonyldiphenol. That is to say, the magnetite nanoparticles are neither simply attached on the outer surface nor encapsulated inside the hollow structure of the nanotubes, but embedded in the walls. Compared with previous studies, the synthesized magnetic PZS nanotubes have the advantages of both surface polymer structure for covalent linkage to biomolecules and hollow structure for encapsulating various drugs together with good magnetic properties. These advantages make these magnetic PZS nanotubes have a bright prospect in applications of catalysis, targeted drug delivery and other bionanotechnology.

Experimental

Hexachlorocyclotriphosphazene (HCCP) (Aldrich) was recrystallized from dry hexane followed by sublimation two times. The melting point of the purified HCCP was 113–114 °C. Triethylamine (TEA), ethanol, sodium hydroxide (NaOH), ferrous chloride tetrahydrate ($FeCl_2{\cdot}4H_2O$), and ferric chloride hexahydrate ($FeCl_3{\cdot}6H_2O$) were purchased from Shanghai Chemical Reagents Corp. (Shanghai, China) and used without further purification. 4,4′-Sulfonyldiphenol (BPS) was purchased from Jiangsu Alonda High-Tech Industry Co., Ltd (Jiangsu, China). Sodium oleate and tetrahydrofuran (THF) were purchased from Sinopharm Chemical Reagent Co., Ltd (Shanghai, China). THF was distilled over sodium under a dry nitrogen atmosphere before use. Deionized water was boiled for 30 min to remove oxygen before use.

The preparation of magnetite nanoparticles was followed by a co-precipitation method. 0.25 g $FeCl_3{\cdot}6H_2O$ and 0.1 g $FeCl_2{\cdot}4H_2O$ were dissolved in 50 mL deionized water by ultrasonic irradiation at high power (150 W, 80 kHz) at room

[a] *School of Chemistry and Chemical Engineering, Shanghai Jiao Tong University, 800 Dongchuan Road, Shanghai, 200240, China. E-mail: xbhuang@sjtu.edu.cn; Fax: +86-21-54741297; Tel: +86-21-54747142*
[b] *National Key Laboratory of Metallic Matrix Composite Material, Shanghai Jiao Tong University, 800 Dongchuan Road, Shanghai, 200240, China. E-mail: xtang@sjtu.edu.cn; Fax: +86-21-54741297; Tel: +86-21-54747142*

† Electronic supplementary information (ESI) available: Table S1 showing the details of the products with different reaction ratios and Fig. S1 showing the SEM images of the products with different reaction ratios. See DOI: 10.1039/b9nj00300b

temperature in a 150 mL three-necked round-bottomed flask under nitrogen. When the solid was dissolved well, 25 mL 0.2 mol L^{-1} NaOH aqueous solution was added dropwise within 20 min. Then, about 0.1 g sodium oleate was added. The reaction was kept at 40 °C for 2 h. The black solid was obtained by magnetic separation and washed three times with deionized water and ethanol respectively. The black Fe_3O_4 nanoparticles were dried under vacuum at 50 °C for use in the next step.

The magnetic PZS nanotubes were prepared as follows: in a typical polymerization system, 0.05 g (0.21 mmol) Fe_3O_4 nanoparticles were dispersed in 100 mL THF by ultrasonic irradiation at high power (150 W, 80 kHz) at room temperature in a 150 mL three-necked round-bottomed flask. After the Fe_3O_4 nanoparticles were dispersed well, the power of ultrasonic irradiation was turned down to 50 W. And then, 0.5 g (1.44 mmol) HCCP, 1.08 g (4.32 mmol) BPS and 5 mL TEA were added in turn. The reaction was kept in an ultrasonic bath at 50 W at room temperature for 8 h. The resultant product was obtained by centrifugation and then washed with THF, deionized water and ethanol in turn several times, respectively. The solid was dried under vacuum at 50 °C to yield magnetic powders.

The Fourier transform IR (FT-IR) spectroscopy was measured on a Perkin-Elmer Paragon 1000 Fourier-transform spectrometer at room temperature (25 °C). The morphology of the magnetic PZS nanotubes was recorded on a JEOL JSM-7401F field emission scanning electron microscope (FE-SEM) at an activation voltage of 5 kV. High resolution transmission electron microscopy (HR-TEM) images were obtained on a JEOL JEM-100CX transmission electron microscope by placing one drop of the samples which were well dispersed in ethanol on copper grids coated with carbon. The elemental analysis was performed by energy dispersive X-ray spectroscopy (EDX) (Hitachi H-9000NAR) equipped with TEM. X-Ray diffraction (XRD) patterns were recorded by using a Bruker D8 Advance instrument equipped with CuKα radiation performed at 40 kV and 40 mA. Thermogravimetric analysis (TGA) was performed on a Perkin Elmer TGA 7/DX thermogravimetric analyzer under a flowing oxygen atmosphere at a scan rate of 10 °C min^{-1} between 50 and 800 °C. The magnetic studies of the magnetic nanotubes were carried out with a vibrating-sample magnetometer (VSM) on a physical properties measurement system at room temperature (25 °C).

Results and discussion

The crystalline structures of the products were studied by XRD. The XRD pattern for magnetic PZS nanotubes is shown in Fig. 1. The magnetite nanoparticles synthesized and pure PZS nanotubes are also shown for comparison. As shown in Fig. 1(a), the characteristic diffraction peaks for the synthesized magnetite nanoparticles are observed. The peaks of 30.2°, 34.6°, 43.0°, 53.2°, 57.3°, 63.0° correspond to the crystal planes of (220), (311), (400), (422), (511) and (440) of crystalline face-centered cubic Fe_3O_4 nanoparticles, which are also in accordance with JCPDS 75-1609. Fig. 1(b) presents the characteristic diffraction peaks for magnetic PZS nanotubes. It

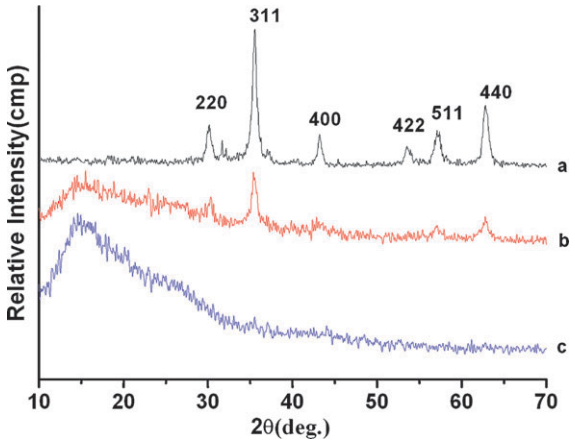

Fig. 1 XRD of (a) Fe_3O_4, (b) magnetic PZS nanotubes, and (c) PZS nanotubes.

is obvious that the magnetic PZS nanotubes have the main characteristic diffraction peaks of magnetite nanoparticles. This confirms the existence of Fe_3O_4 nanoparticles. The very broad diffraction peak at 2θ values around 15.0° corresponds to the reflection peak position of pure PZS nanotubes, according to the similar peak in Fig. 1(c). The intensities of the peaks are relatively lower and the peaks are a little wider than the pure magnetite nanoparticles, caused by abundant PZS polymers interacting with Fe_3O_4 nanoparticles.

The morphology and structure of magnetite nanoparticles and the magnetic PZS nanotubes were investigated by FE-SEM and HR-TEM. Fig. 2(a) displays a SEM image of the magnetic PZS nanotubes. The magnetic PZS nanotubes are several microns in length and 50–100 nm in outer diameter. Some nanotubes possess branch nanostructures by the fact that two nanotubes are coherent with each other at the bottom. Fig. 2(b) presents the TEM image of magnetite

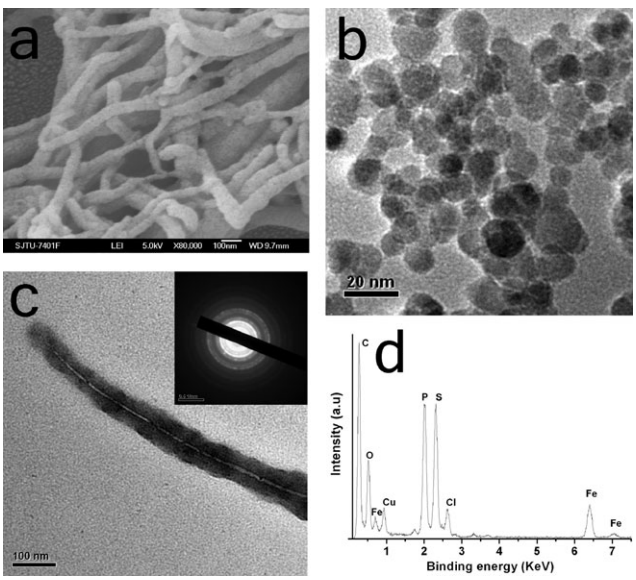

Fig. 2 SEM images of (a) magnetic PZS nanotubes; HR-TEM images of (b) Fe_3O_4 nanoparticles, (c) magnetic PZS nanotubes, the inset shows the ED pattern taken of the nanotubes; (d) EDX of magnetic PZS nanotubes.

nanoparticles. It indicates that magnetite nanoparticles of 5–10 nm in diameter were successfully synthesized. Fig. 2(c) depicts the TEM image of the magnetic PZS nanotubes. It shows that the magnetic nanotubes are 50–100 nm in outer diameter and 5–10 nm in inner diameter with hollow tubular structures. The darker regions in the walls in the image are caused by the presence of magnetite nanoparticles. The selected area electron diffraction (SAED) pattern inserted in Fig. 2(c) corresponding to the darker region confirms the existence of inorganic crystalline magnetite in the walls. EDX measurement also suggests the presence of the magnetite nanoparticles. As shown in Fig. 2(d), the local elemental composition of the magnetic PZS nanotubes was analyzed. The EDX spectrum containing elemental iron, carbon, sulfur, phosphorus, chlorine and oxygen indicates that the magnetic nanotubes are composed of PZS and Fe_3O_4.

The chemical structure of magnetic PZS nanotubes was determined by FT-IR spectroscopy. The results are shown in Fig. 3(a). The FT-IR spectrum of pure PZS nanotubes is shown in Fig. 3(b) for comparison. Scheme 1 displays the polymerisation reaction and chemical structure of PZS. It is obvious that the magnetic nanotubes have all of the characteristic peaks of PZS nanotubes. The peaks at 1244 and 1187 cm^{-1} correspond to the stretching vibrations of P═N and 883 cm^{-1} corresponds to P–N groups in the cyclotriphosphazene structure, respectively. The peaks at 1325, 1289 and 1154 cm^{-1} are assigned to the O═S═O stretching vibrations of the sulfonylphenol units. Two peaks at 1585 and 1488 cm^{-1} are the C═C stretching vibrations in the phenylene of sulfonylphenol units. The absorption at 943 cm^{-1} is ascribed to P–O–(Ph) which is obvious evidence of polymerization of the monomers HCCP and BPS. The absorption of inorganic magnetite nanoparticles is relatively weak and basically covered by the PZS nanotubes in the FT-IR spectrum.

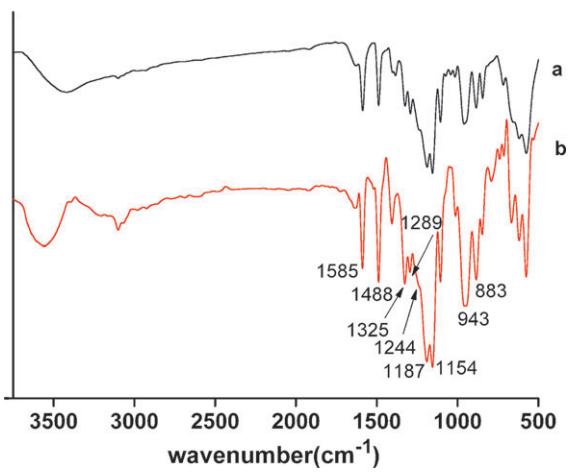

Fig. 3 FT-IR spectra of (a) magnetic PZS nanotubes and (b) pure PZS nanotubes.

A possible formation mechanism of the magnetic PZS nanotubes with magnetic phases embedded in the walls was proposed based on our previous study about the synthesis of PZS nanotubes,[16] as shown in Fig. 4. The polycondensation of HCCP and equimolar BPS with excess TEA as a catalyst generated primary polymer particles and hydrogen chloride (HCl). The HCl combined with excess TEA to form the primary template nanocrystals (TEACl) which can grow along their axes to form a nanometre-sized rodlike structure. Under ultrasonic irradiation, the primary polymer particles first adhered onto the surface of the magnetite nanoparticles which exist in the system. As the polymerization proceeded, TEACl was precipitated to form a template. Because of the high surface energy of the TEACl nanocrystals, the primary polymer particles together with the attached magnetite nanoparticles adhered onto the surface of the template. At last, the TEACl nanocrystals inside the cavity of the products were removed by washing with water to obtain the magnetic PZS nanotubes.

According to the above proposal, the key to successful synthesis depends on whether the primary polymer particles, once adhered onto the surface of the magnetite nanoparticles, can adhere onto the templates to form the one-dimensional nanostructure. The experimental results show that only when the concentration of the reactants is within certain limits, can the magnetic PZS nanotubes be successfully obtained. The morphology of the magnetic PZS nanotubes is highly influenced by the content of Fe_3O_4 nanoparticles, which is shown in the ESI (Fig. S1 and Table S1†).

The TGA of the magnetic PZS nanotubes was performed over the temperature range of 50–800 °C under a flowing oxygen atmosphere and that of the pure PZS nanotubes was used for comparison, as shown in Fig. 5. The results show that the magnetic PZS nanotubes have a high onset of the thermal-degradation temperature of about 400 °C, exhibiting good thermal stability, as shown in Fig. 5(a). However, the onset is about 50 °C lower than that of the pure PZS nanotubes (as shown in Fig. 5(b)) probably because the magnetite nanoparticles may catalyze the oxidation of PZS nanotubes at a lower temperature.[17,18] The residues after decomposition of the samples in oxygen at 800 °C were identified as Fe_2O_3. According to the residual ratio of about

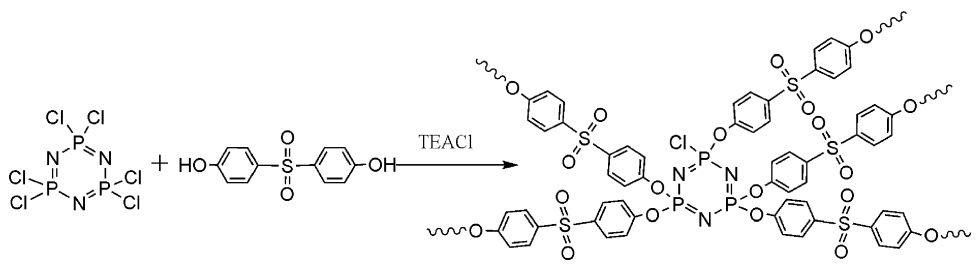

Scheme 1 Polymerisation reaction and chemical structure of PZS.

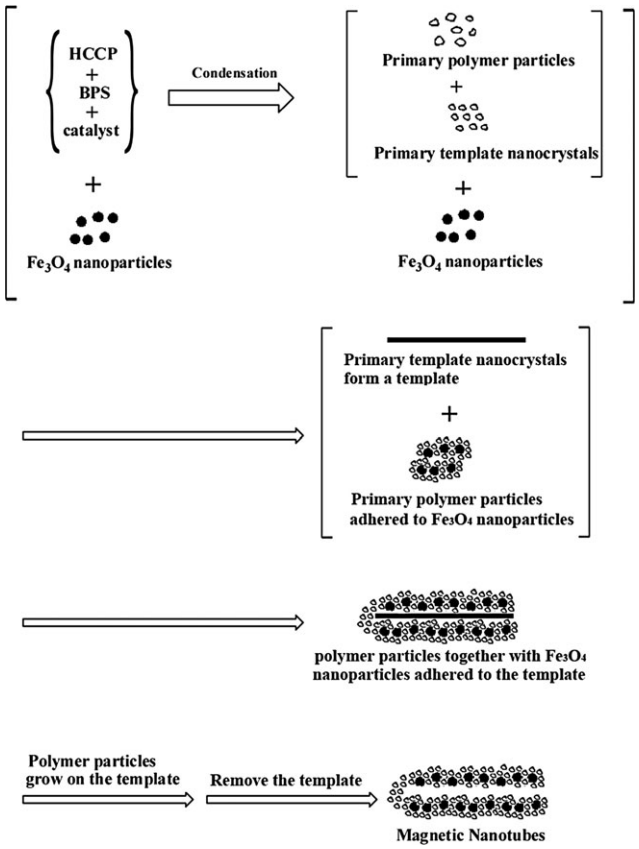

Fig. 4 Schematic illustration of the procedure for the synthesis of the magnetic PZS nanotubes with magnetic phases embedded in the walls.

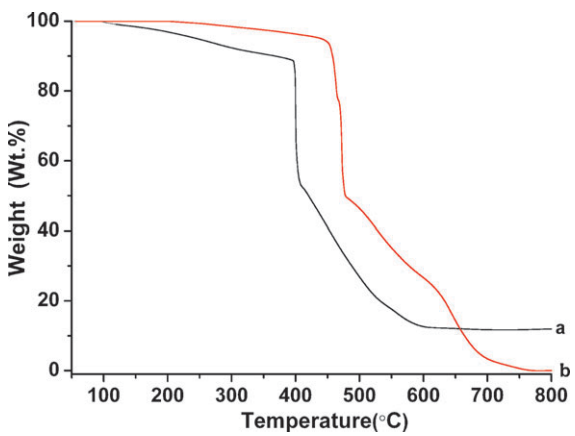

Fig. 5 TGA curve under a flowing oxygen atmosphere for: (a) magnetic PZS nanotubes, and (b) PZS nanotubes.

11.9%, the magnetism content calculated of the magnetic PZS is about 11.5%.

Fig. 6(a) shows the M–H hysteresis loop measured for magnetic PZS nanotubes at 25 °C. It indicates that the magnetic PZS nanotubes exhibit good magnetic properties with a saturation magnetization, M_s = 2.68 emu g^{-1}. Nearly no remnant magnetization (M_r = 0.06 emu g^{-1}) and very small coercive field (H_c = 9.9 Oe) from the hysteresis loops at a low applied magnetic field (as shown in Fig. 6(b)) show that the magnetic PZS nanotubes exhibit superparamagnetic

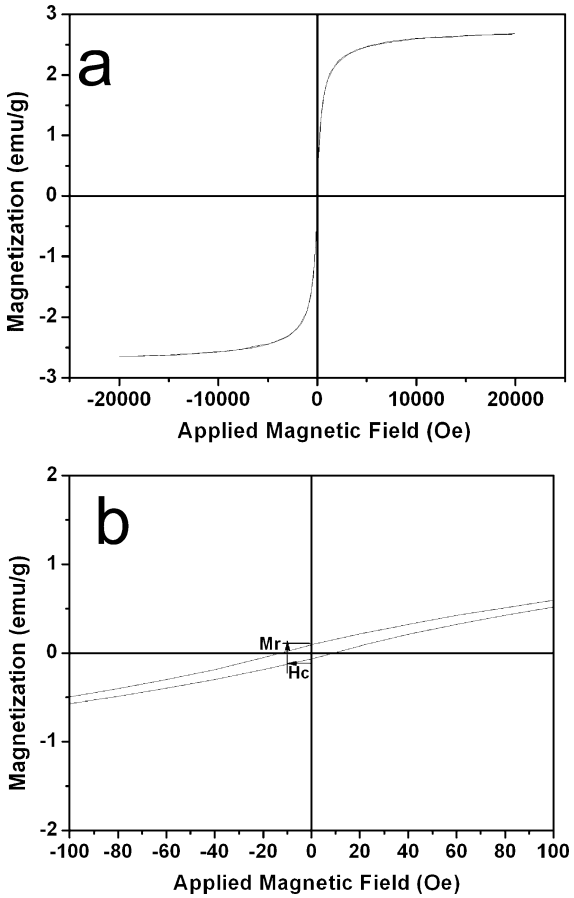

Fig. 6 (a) The *M–H* hysteresis loop measured for magnetic PZS nanotubes at 25 °C and (b) a magnified view of the magnetization curves at low applied fields.

properties at 25 °C and have nearly no remanence effects. The superparamagnetic properties are attributed to the small size of the Fe_3O_4 nanoparticles.

Conclusions

In summary, we have successfully synthesized magnetic PZS nanotubes with magnetic phases embedded in the walls by ultrasonic irradiation *via* an *in situ* template approach. The magnetic PZS nanotubes are several microns in length, 50–100 nm in outer diameter and 5–10 nm in inner diameter. The magnetite nanoparticles that take part in the formation of the magnetic nanotubes are embedded in the walls of the nanotubes. The morphology of the magnetic PZS nanotubes is highly influenced by the content of Fe_3O_4 nanoparticles. The characteristic results show that the magnetic PZS nanotubes have good thermal stability and superparamagnetic properties. The magnetic PZS nanotubes, which have both surface polymer structure for covalent linkage to biomolecules and hollow structure for encapsulating various drugs, will have promising applications in catalysis, targeted drug delivery and other bionanotechnology.

Acknowledgements

This work was supported by the Shanghai Leading Academic Discipline Project, Project Number: B202.

References

1 G. D. Moeser, W. H. Green, P. E. Laibinis, P. Linse and T. A. Hatton, *Langmuir*, 2004, **20**, 5223–5234.
2 F. Caruso, M. Spasova, A. Susha, M. Giersig and R. A. Caruso, *Chem. Mater.*, 2001, **13**, 109–116.
3 T. Hyeon, S. S. Lee, J. Park, Y. Chung and H. Bin Na, *J. Am. Chem. Soc.*, 2001, **123**, 12798–12801.
4 S. H. Yu and M. Yoshimura, *Adv. Funct. Mater.*, 2002, **12**, 9–15.
5 J. L. Zhang, Y. Wang, H. Ji, Y. G. Wei, N. Z. Wu, B. J. Zuo and Q. L. Wang, *J. Catal.*, 2005, **229**, 114–118.
6 H. Zeng, J. Li, J. P. Liu, Z. L. Wang and S. H. Sun, *Nature*, 2002, **420**, 395–398.
7 R. C. Wu, J. H. Qu and Y. S. Chen, *Water Res.*, 2005, **39**, 630–638.
8 G. Korneva, H. H. Ye, Y. Gogotsi, D. Halverson, G. Friedman, J. C. Bradley and K. G. Kornev, *Nano Lett.*, 2005, **5**, 879–884.
9 S. J. Son, J. Reichel, B. He, M. Schuchman and S. B. Lee, *J. Am. Chem. Soc.*, 2005, **127**, 7316–7317.
10 C. N. He, F. Tian, S. J. Liu, Z. J. Diu, C. J. Liu, F. Li and S. Q. Chen, *Mater. Lett.*, 2008, **62**, 3697–3699.
11 H. Q. Wu, Y. J. Cao, P. S. Yuan, H. Y. Xu and X. W. Wei, *Chem. Phys. Lett.*, 2005, **406**, 148–153.
12 C. Gao, W. W. Li, H. Morimoto, Y. Nagaoka and T. Maekawa, *J. Phys. Chem. B*, 2006, **110**, 7213–7220.
13 Z. P. Dong, K. Ma, J. G. He, J. J. Wang, R. Li and J. T. Ma, *Mater. Lett.*, 2008, **62**, 4059–4061.
14 F. Zhang and C. C. Wang, *J. Phys. Chem. C*, 2008, **112**, 15151–15156.
15 X. Y. Zhang, X. B. Huang and X. Z. Tang, *J. Mater. Chem.*, 2009, **19**, 3281–3285.
16 L. Zhu, Y. Y. Xu, W. Z. Yuan, J. Y. Xi, X. B. Huang, X. Z. Tang and S. X. Zheng, *Adv. Mater.*, 2006, **18**, 2997–3000.
17 R. K. Rana, X. N. Xu, Y. Yeshurun and A. Gedanken, *J. Phys. Chem. B*, 2002, **106**, 4079–4084.
18 L. Zhang, L. Chen and Q. H. Wan, *Chem. Mater.*, 2008, **20**, 3345–3353.

